昭和47年2月15日　第3種郵便物認可　平成25年3月5日発行(毎月5日発行)通巻495号　ISSN 0366-7022

Chemistry Letters

Highlight Review

Luminescent Complexes Containing Halogeno-bridged Dicopper(I) Unit $\{Cu_2(\mu\text{-}X)_2\}$(X = Cl, Br, and I)
Kiyoshi Tsuge

Vol. 42 No. 3 2013
CMLTAG 203-326 (2013)
MARCH 5, 2013

The Chemical Society of Japan

Chemistry Letters

http://www.csj.jp/journals/chem-lett/

Vol.42 No.3
March, 2013

CMLTAG
ISSN 0366-7022

Highlight Review

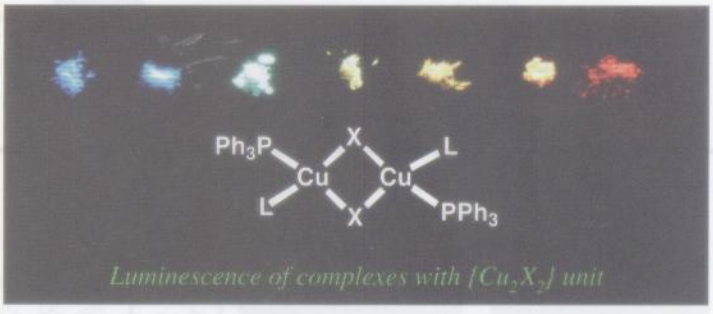

Luminescence of complexes with $\{Cu_2X_2\}$ unit

Kiyoshi Tsuge
doi:10.1246/cl.2013.204

Luminescent copper(I) complexes have been extensively studied in these decades with various ligands showing their rich photophysical and photochemical properties. In this contribution, the luminescent halogeno copper(I) complexes, especially those with halogeno-bridged dicopper(I) unit $\{Cu_2(\mu\text{-}X)_2\}$, one of the basic, common structural motifs among halogeno copper(I) family, are described from the view point of influences of coligands upon their luminescent properties. Discussions are extended to the complexes with the halogeno-bridged tetranuclear unit $\{Cu_4(\mu_3\text{-}X)_4\}$, being another common structural motif, to examine the dominant emissive excited states in halogeno copper(I) complexes.

Letter

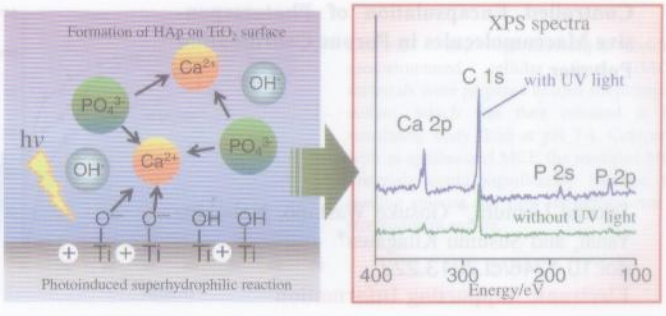

Tsuyoshi Sugita, Masanobu Mori,* Hisashi Nakane, Akinori Mase, and Hideyuki Itabashi
doi:10.1246/cl.2013.209
Electronic Supporting Information

224 **Synthesis, Characterization, and Optical Properties of $Zn_{1-x}Co_xO$ Nanostructures**

Lu-Ping Zhu,* Hua Huang, Ling-Ling Wang, Nai-Ci Bing, Gui-Hong Liao, and Li-Jun Wang*

doi:10.1246/cl.2013.224

Co doping can enhance the ability of visible light absorption of the ZnO samples, and the band gap energies of the $Zn_{1-x}Co_xO$ nanostructures can be effectively tuned from 3.25 to 2.85 eV.

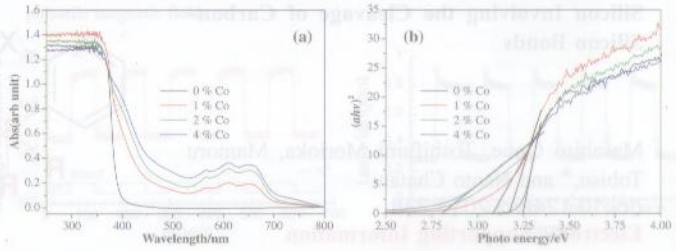

227 **Design and Synthesis of Novel Piperazine Derivatives with High Antibacterial Activity**

Maolan Zhang, Yuanliang Wang,* Jiaoxia Sun, Jinchuan Wu, Weiwei Yan, and Yuxi Zheng

doi:10.1246/cl.2013.227

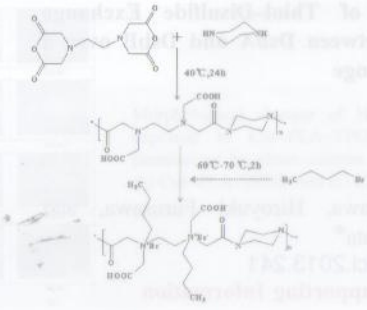

229 **Effect of Optical Purity of C_3-Symmetric Chiral Tris-ureas on Supramolecular Gel Formation**

Tomoe Nakagawa, Mawo Amakatsu, Kanako Munenobu, Hiromitsu Fujii, and Masamichi Yamanaka*

doi:10.1246/cl.2013.229

Electronic Supporting Information

232 **Room-temperature Sinterable Silver Nanoparticle Ink with Low-molecular-weight Poly(*N*-vinylpyrrolidone) Ligand**

Mi Yeon Lee, Won Jin Lee, Arup Kumer Roy, Kang Seok Lee, Sung Young Park,* Ji-Hoon Lee,* and Insik In*

doi:10.1246/cl.2013.232

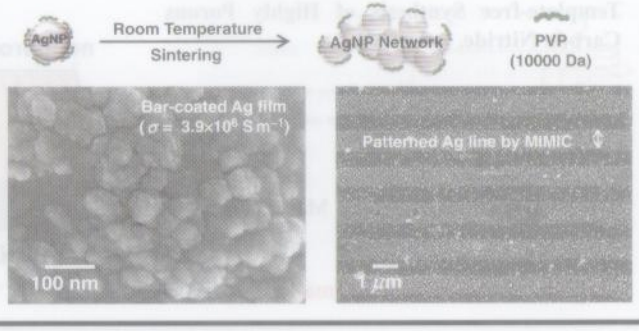

235 **Functionalized Mesostructured Cellular Foams for Loading and Release of Streptomycin**

Shaohua Xu, Jiawey Yong, Guosong Lai, Haili Zhang, Yiwei Wu, and Aimin Yu*

doi:10.1246/cl.2013.235

Electronic Supporting Information

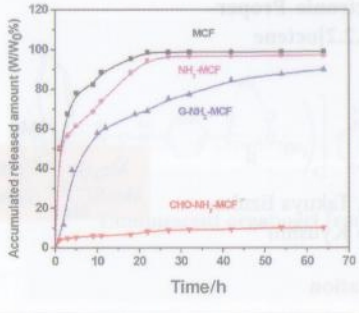

Glucose- and glutaraldehyde-modified mesostructured cellular foam (MCF) materials were prepared to load streptomycin sulfate, which was then released in the simulating body fluid at pH 7.4. Compared with as-synthesized MCF, the modified MCF materials could significantly increase the loading amount and slow the release rate of streptomycin sulfate.

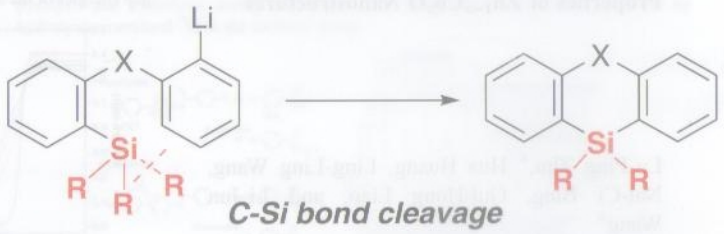

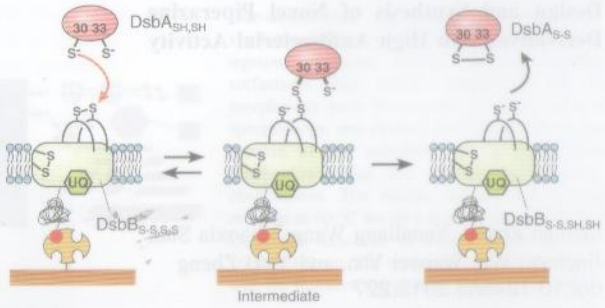

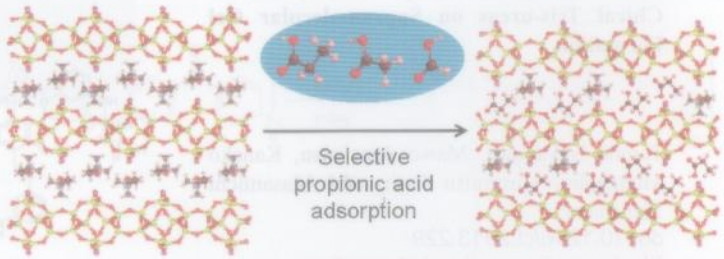

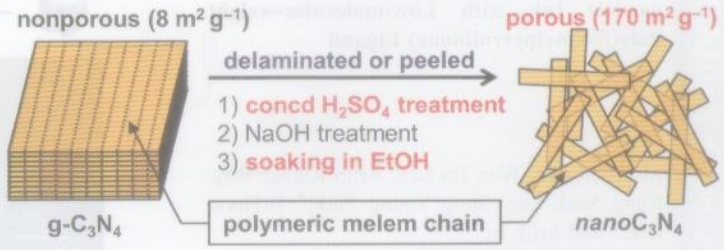

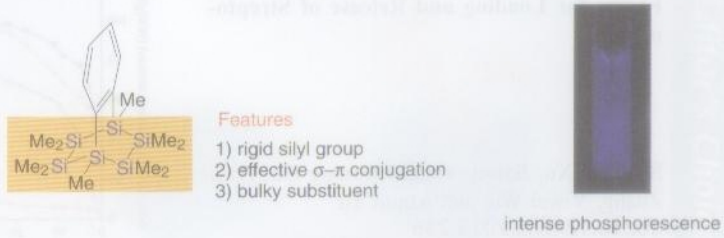

253 **Wide-range Modulation of Dynamic Modulus and Loss Tangent for Magnetic Elastomers Containing Submilimeter Magnetic Particles**

Naoya Chiba, Ken Yamamoto, Tsukasa Hojo, Mika Kawai, and Tetsu Mitsumata*
doi:10.1246/cl.2013.253

Magnetic elastomers embedded with submillimeter magnetic particles exhibit giant magnetoelastic behavior. The storage modulus and loss tangent altered in response to a pulsatile magnetic field.

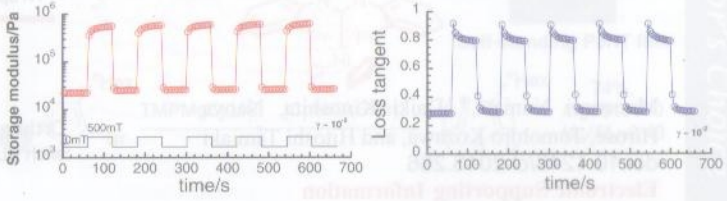

255 **In Vitro Apoptosis Enhancement of Hep-G2 Cells by PLA–TPGS and PLA–PEG Block Copolymer Encapsulated Curcumin Nanoparticles**

Ha Phuong Thu,* Duong Tuan Quang, Mai Thi Thu Trang, Tran Thi Hong Ha, Nguyen Hoai Nam, Nguyen Xuan Phuc, Tran Thi Minh Nguyet, Phan Quoc Thong, Phan Thi Hong Tuyet, Vuong Thi Kim Oanh, and Le Mai Huong*
doi:10.1246/cl.2013.255
Electronic Supporting Information

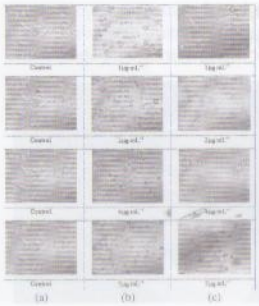

Morphological changes of Hep-G2 cells upon their exposure to Cur–PLA–TPGS and Cur–PLA–PEG monitorized by phase-contrast microscope: (a) Control, (b) Cur–PLA–TPGS, and (c) Cur–PLA–PEG.

258 **A Carbon/Iron–Cerium/Alumina Catalyst as Potential Substitution for Noble Metal Three-way Catalyst for Auto Emission Control**

Yu Guo,* Harunobu Oda, Lu Jia, Shuntaro Amari, Yui Okita, and Hideo Kameyama
doi:10.1246/cl.2013.258

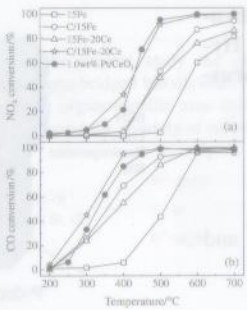

When the alumina-supported Fe and Ce catalyst was subjected to a carburization treatment (i.e. C/15Fe–Ce), it exhibited a dramatic activity for removing NO_x and CO, because the initial temperature for NO_x reduction was shifted to 300 °C and 95% conversion of CO and NO_x could be achieved at 500 °C, even comparable to a reference noble metal catalyst 1.0 wt % Pt/CeO_2.

261 **Remarkable Enhancement of Sensitivity with the Second Generation of Elliptically Polarization-detected Circular Dichroism Spectroscopy**

Makoto Murakami, Yasuyuki Araki,* Seiji Sakamoto, Yoshiki Hamada, and Takehiko Wada*
doi:10.1246/cl.2013.261
Electronic Supporting Information

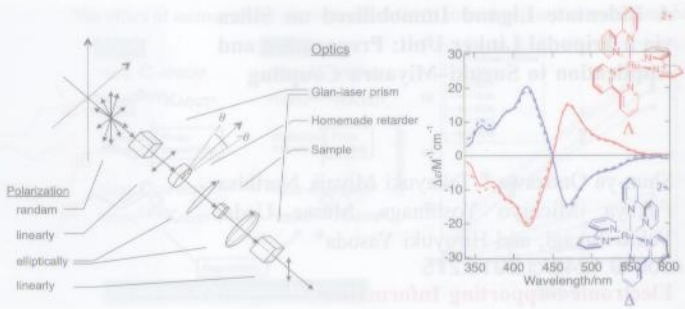

Editor's Choice

263 **Formation of Luminescent Organogels from Europium-based Complexes**

Akihiko Tsuge,* Daisuke Yakeya, Katsuhiko Sakura, Tetsuji Moriguchi, Daisaku Kaneko, Takahide Kanyama, Takayoshi Kawahara, and Koji Araki
doi:10.1246/cl.2013.263
Electronic Supporting Information

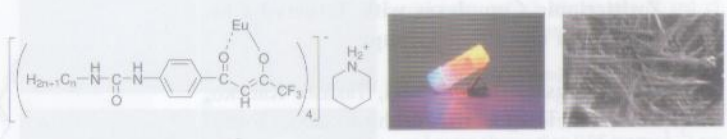

Luminescent organogel from the europium-based complex

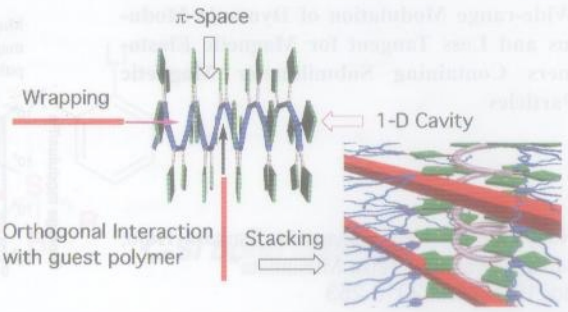

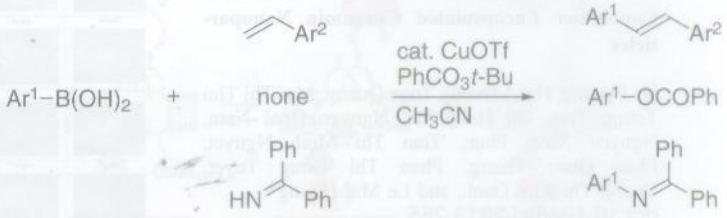

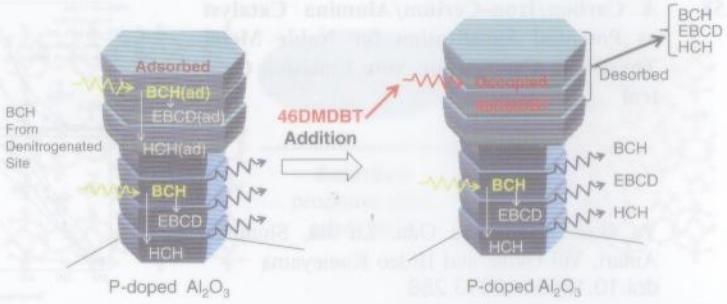

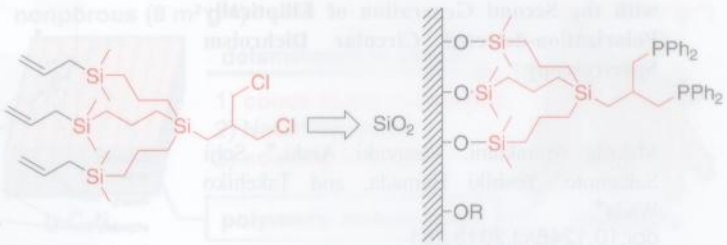

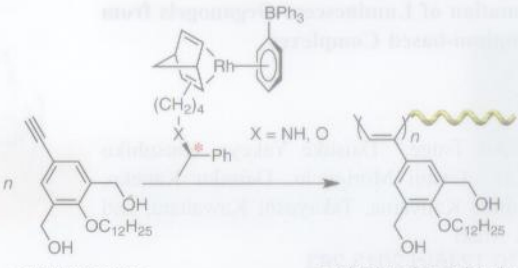

Editor's Choice

281 **Synthesis of High-molecular-weight Head-to-tail-type Poly(3-substituted-thiophene)s by Cross-coupling Polycondensation with [CpNiCl(NHC)] as a Catalyst**

Shunsuke Tamba, Kanta Fuji, Hikaru Meguro, Shuji Okamoto, Tadashi Tendo, Ryo Komobuchi, Atsushi Sugie, Takashi Nishino, and Atsunori Mori*

doi:10.1246/cl.2013.281

Electronic Supporting Information

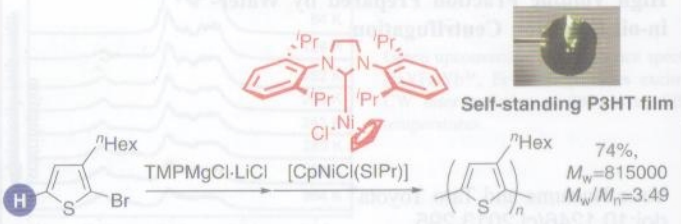

284 **Friction Evaluation System with a Human Finger Model**

Keitaro Kuramitsu, Toshio Nomura, Shyuhei Nomura, Takashi Maeno, and Yoshimune Nonomura*

doi:10.1246/cl.2013.284

Electronic Supporting Information

We developed a friction evaluation system with a human finger model. The surface of the model was covered with imitation fingerprints. When a polypropylene surface was rubbed against the finger model, the friction profile varied with the sliding velocity and vertical force.

286 **Application of a Bis(silylene) Nickel Complex as Precatalyst in C–C Bond Formation Reactions**

Chika I. Someya, Michael Haberberger, Wenyuan Wang, Stephan Enthaler,* and Shigeyoshi Inoue*

doi:10.1246/cl.2013.286

In the present study the catalytic performance of a nickel complex stabilized by an oxygen-bridged bis(silylene) ligand was examined in cross-coupling reactions of aryl halides with organometallic zinc and Grignard reagents. Good to excellent catalytic activity was observed for a variety of substrates with this system.

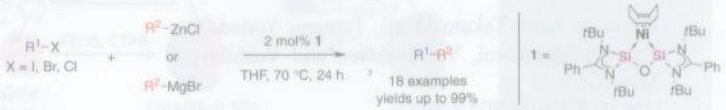

289 **Diamine Derivatives Accelerate Photochemical C → U Transition in DNA Double Strand**

Kenzo Fujimoto,* Daiki Futamura, and Takashi Sakamoto

doi:10.1246/cl.2013.289

Electronic Supporting Information

The effect of amines on the photochemical C→U transition reaction was examined.

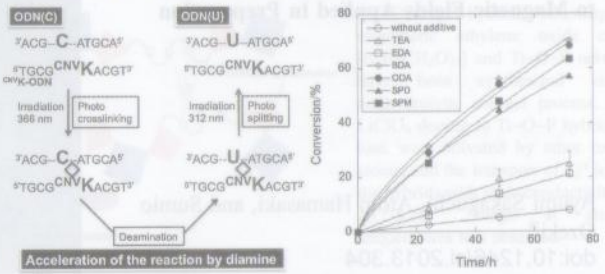

292 **Hydration of Adamantane Skeleton: Water Assembling around Amantadine and Halo-substituted Adamantanes**

Hideo Doi and Misako Aida*

doi:10.1246/cl.2013.292

Electronic Supporting Information

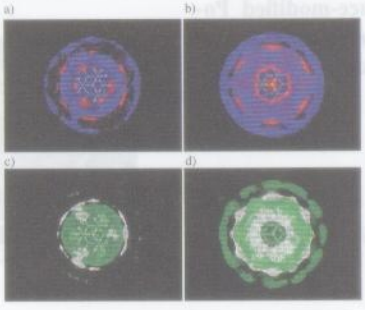

Oxygen (a and b) and hydrogen (c and d) number density maps of solvent water molecules around adamantane (a and c) and perfluoroadamantane (b and d). For O number density, red (higher than 0.09 atoms $Å^{-3}$) and blue (lower than 0.02 atoms $Å^{-3}$) are plotted; for H number density, white (higher than 0.12 atoms $Å^{-3}$) and green (lower than 0.05 atoms $Å^{-3}$) are plotted. Note that O number density of bulk water (1 g cm^{-3}) is uniform and 0.033 atoms $Å^{-3}$.

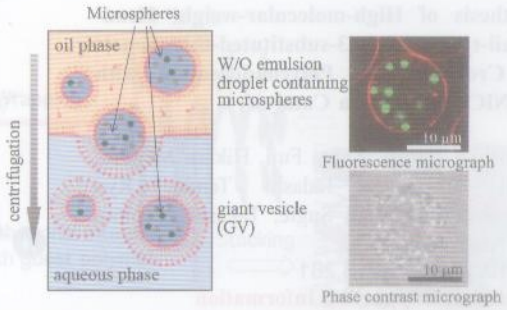

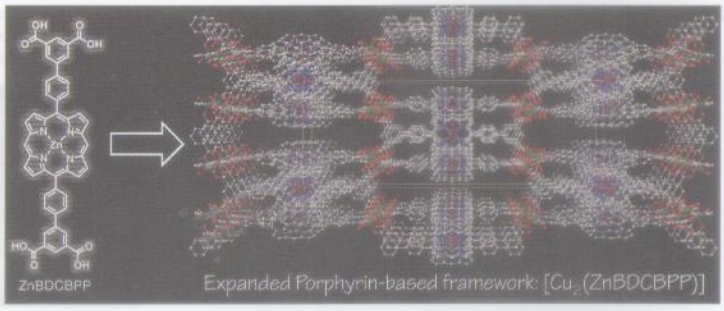

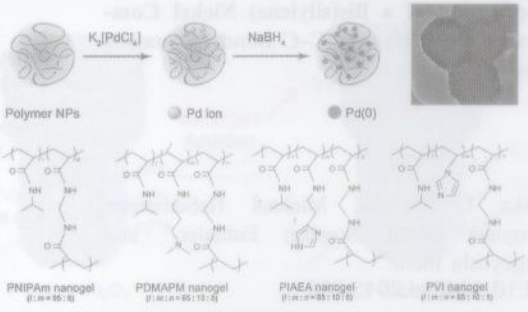

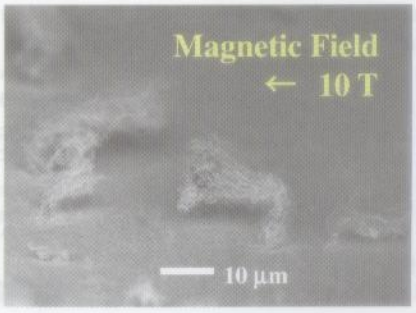

Magnetic orientation of multiwalled carbon nanotube bundles.

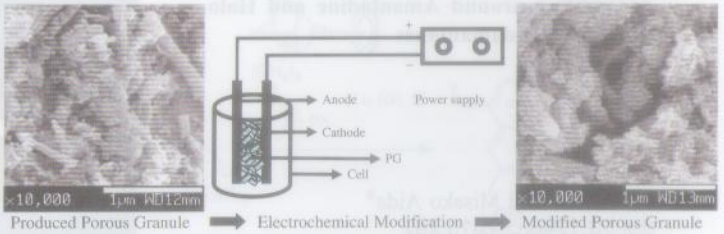

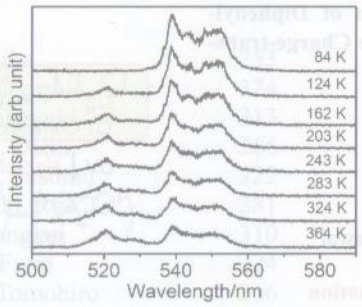

Green upconversion luminescence spectra of $NaYF_4$:Yb^{3+}, Er^{3+} nanoparticles excited by CW laser radiation at 980 nm at different temperatures.

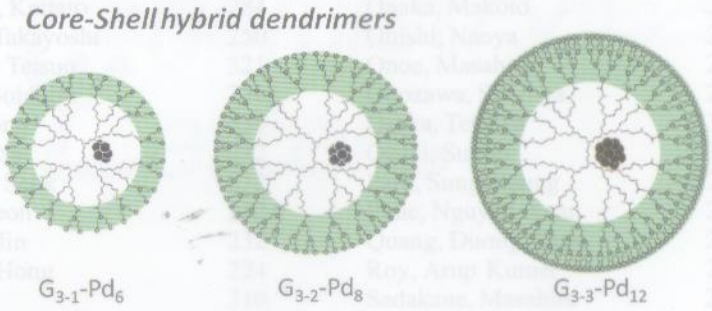

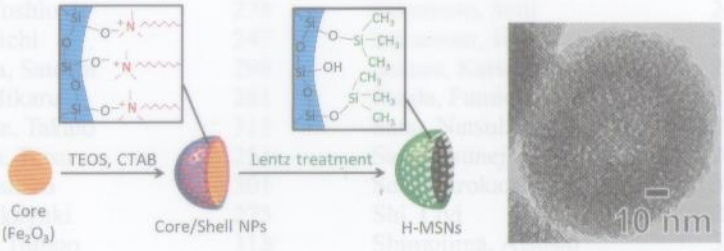

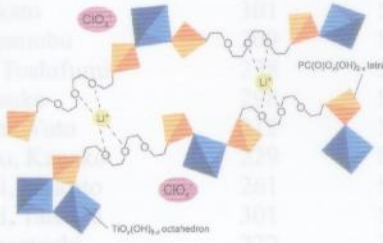

$LiClO_4$-doped hybrids possessing both oligomeric ethylene oxide chains [$(CH_2CH_2O)_3$] and Ti–O–P networks have been synthesized via a nonhydrolytic sol–gel process. After $LiClO_4$ doping to Ti–O–P hybrid, Li^+ ions were solvated by ether oxygen atoms, and the transport of Li^+ ions in the hybrids with ionic conductivities at 10^{-5} S cm^{-1} range at ambient temperatures was observed.

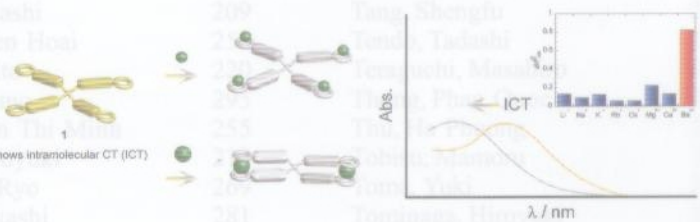

324 **Efficient Photopolymerization of Diphenylamine Based on Ground-state Charge-transfer Complex**

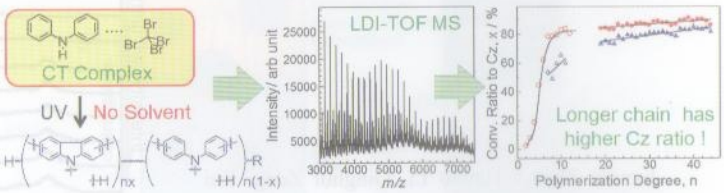

Fumi Koyama and Tsuyoshi Kawai*
doi:10.1246/cl.2013.324
Electronic Supporting Information

